the dry nitrogen atmosphere of a glovebox. Reactions involving NF_4^+ salts were carried out in $^3/_4$ in. o.d. Teflon-FEP ampules closed by a stainless steel valve.

The ^{19}F and ^1H NMR spectra were measured at 84.6 and 90 MHz, respectively, on a Varian Model EM390 spectrometer, with 4-mm Teflon-FEP tubes (Wilmad Glass Co.) as sample containers and $CFCl_3$ and TMS, respectively, as internal standards, with negative shifts being upfield from the standards. Raman spectra were recorded on either a Cary Model 83 or a Spex Model 1403 spectrophotometer by use of the 488-nm exciting line of an Ar ion or the 647.1-nm line of a Kr ion laser, respectively. Baked-out Pyrex melting point capillaries were used as sample holders. Infrared spectra were recorded on a Perkin-Elmer Model 283 spectrophotometer as AgCl disks that were pressed in a Wilks minipress inside the drybox.

The NF_4BF_4–$N(CH_3)_4F$–CH_3CN System. NF_4BF_4 (0.54 mmol) and $N(CH_3)_4F$ (0.60 mmol) were loaded inside the drybox into a $^3/_4$ in. Teflon-FEP ampule. On the vacuum line, dry CH_3CN (3 mL liquid) was added at −196 °C, and the mixture was warmed to −31 °C for 30 min. The ampule was cooled to −78 °C, and the volatile material (0.45 mmol) was expanded into the vacuum line and shown by fractional condensation at −210 °C and infrared spectroscopy to consist mainly of NF_3 (0.40 mmol). The mixture in the ampule was then warmed for 3 h to −31 °C and for 1 h to room temperature, and an additional amount of NF_3 (0.13 mmol) was evolved. The solid residue (90.9 mg, weight calculated for 0.54 mmol of $N(CH_3)_4BF_4$ and 0.06 mmol of unreacted $N(CH_3)_4F$ = 92.9 mg) was shown by vibrational spectroscopy to consist mainly of $N(CH_3)_4BF_4$. When the reaction was repeated using a 5-fold excess of $N(CH_3)_4F$ at −31 °C, the NF_3 evolution was 95% complete after 30 min.

The NF_4BF_4–$N(CH_3)_4F$–CHF_3 System. NF_4BF_4 (2.19 mmol) and $N(CH_3)_4F$ (2.24 mmol) were combined in a Teflon ampule, and CHF_3 (50.26 mmol) was added at −196 °C. The mixture was warmed to −78 °C for 3 h and then cooled again to −196 °C, and the noncondensable gases (0.45 mmol of F_2) were measured. Subsequently, the ampule was warmed to the melting point of CHF_3 (−155 °C), and the volatile material was removed in a dynamic vacuum by fractional condensation through traps kept at −186 and −210 °C. The −210 °C trap contained NF_3 (2.16 mmol). The solid residue, after being pumped on at room temperature (360 mg), consisted mainly of $N(CH_3)_4BF_4$ (weight calculated for 2.19 mmol of $N(CH_3)_4BF_4$ and 0.05 mmol $N(CH_3)_4F$ = 357 mg). When the reaction was repeated at −142 °C, only 10% of the theoretical amount of NF_3 was evolved in 3 h.

Acknowledgment. The authors are grateful to Dr. Carl J. Schack and Mr. R. D. Wilson for help and to the Air Force Phillips Laboratory and the U.S. Army Research Office for financial support.

Conformation of Two 4′-Thio-2′-deoxynucleoside Analogs Studied by 500-MHz ^1H NMR Spectroscopy and X-ray Crystallography

Leo H. Koole,[†] Janez Plavec,[†] Hongying Liu,[‡] Beverly R. Vincent,[‡] Michael R. Dyson,[§] Paul L. Coe,[§] Richard T. Walker,[§] George W. Hardy,[⊥] S. George Rahim,[⊥] and Jyoti Chattopadhyaya*,[†]

Contribution from the Department of Bioorganic Chemistry, Box 581, Biomedical Centre, University of Uppsala, S-751 23 Uppsala, Sweden, Molecular Structure Corporation, 3200 Research Forest Drive, The Woodlands, Texas 77381, School of Chemistry, University of Birmingham, Birmingham B15 2TT, England, and The Wellcome Research Laboratories, Beckenham, Kent BR3 3BS, England. *Received December 23, 1991*

Abstract: An integrated conformational study is reported on the structurally modified nucleosides 4′-thiothymidine (**1**), an isoelectronic analogue of natural thymidine, and (*E*)-5-(2-bromovinyl)-2′-deoxy-4′-thiouridine (**2**). The conformation of **1** and **2** in D_2O solution was inferred from the vicinal proton–proton NMR coupling constants and nuclear Overhauser (nOe) contacts. Significant adaptions of the conventional routines for *J*-coupling analysis in nucleos(t)ide structures were necessary due to the presence of sulfur instead of O4′ in the thiofuranose ring. A pseudorotational equation of the form $\nu_j = a_j\nu_m \cos(P + \epsilon_j + 144°(j-2))$ was used to account for the nonequilateral nature of the 4′-thiofuranose ring. The parameter sets a_0, ..., a_4 and ϵ_0, ..., ϵ_4 were deduced from a set of ab initio (HF/3-21G level) molecular orbital calculations. Analysis of the *J*-coupling constants measured for **1** and **2** revealed that (i) the C4′–C5′ bond is primarily in the γ^+ or γ^t conformation and (ii) the 4′-thiofuranose ring has a preference for a South-type (C2′-endo/C3′-exo) puckered conformation. The preference for the South conformation is slightly larger for **1** (73% at 300 K) than for **2** (66% at 300 K). The pseudorotational parameters of the South conformer are as follows: $P = 177°$, $\nu_m = 43°$ for **1**, and $P = 177°$, $\nu_m = 44°$ for **2**. The results reveal that another conformer with a North-type puckered conformation of the 4′-thiofuranose ring is also present in solution, *to an extent of ≈27% for 1 and 34% for 2 at ambient temperature.* The pseudorotational parameters describing the thiofuranose conformation of the minor conformer are as follows: $P = 13°$, $\nu_m = 45°$ for **1**, and $P = 9°$, $\nu_m = 45°$ for **2**. The characterization of the minor conformer must be regarded as an essential complement to the results of X-ray crystallographic analyses. One-dimensional nOe measurements indicated a predominant anti conformation of the thymine base in **1** and the modified uridine base in **2**. The crystal structures of **1** and **2** were found to be grossly similar. The most important characteristics are as follows: compound **1**, $P = 177.7°$, $\nu_m = 47.9°$, $\chi = -144.7°$, $\gamma = 179.5°$; compound **2**, $P = 179.5°$, $\nu_m = 48.6°$, $\chi = -140.0°$, and $\gamma = 174.1°$. Furthermore, it is concluded that the preferred conformation of **1** and **2** in solution is in close agreement with the X-ray crystal structure. The present results indicate that it is dangerous to rely solely on X-ray crystallographic information in attempts to explain or predict biological activity of modified nucleosides. The best basis for formulating structure–activity relationships for modified nucleosides is probably a combined interpretation of solid state and solution conformational data.

Introduction

The ongoing search for more active and more specific anti-(retro)viral agents has stimulated many investigations on structurally modified nucleosides and nucleotides. A plethora of these compounds is known today.[1] A general conclusion emerging from

[†] University of Uppsala.
[‡] Molecular Structure Corporation.
[§] University of Birmingham.
[⊥] The Wellcome Research Laboratories.

(1) (a) Proceedings of the 9th International Round Table on Nucleosides, Nucleotides and Their Biological Applications, Uppsala, Sweden, 1990: *Nucleosides and Nucleotides* **1991**, *10*, 3–737. (b) *Nucleoside Analogues. Chemistry, Biology and Medical Applications*; Walker, R. T., de Clercq, E., Eckstein, F., Eds.; Plenum Press: New York, 1979.

0002-7863/92/1514-9936$03.00/0

Table I. Experimental $^1H-^1H$ *J*-Coupling Constants at 500 MHz for Compounds **1** and **2** and Thymidine

	1[a]					**2**[b]					thymidine[a]				
coupling	285 K	300 K	313 K	333 K	353 K	285 K	300 K	313 K	333 K	353 K	285 K	300 K	313 K	333 K	353 K
$J_{1'2'}$	8.0	7.8	7.7	7.4	7.3	7.4	7.2	7.2	7.0	6.9	13.6[d,f]	13.6[d,f]	13.6[d,f]	6.7	6.6
$J_{1'2''}$	6.7	6.7	6.8	6.8	6.9	6.8	6.7	6.8	6.8	6.8				6.8	6.8
$J_{2'3'}$	4.2	4.3	4.4	4.6	4.6	4.4	4.4	4.4	4.5	4.6	10.7[e,f]	10.9[e,f]	10.8[e,f]	7.1	7.1
$J_{2''3'}$	4.2	4.4	4.5	4.7	4.9	5.1	5.0	5.1	5.1	5.1				3.9	4.2
$J_{3'4'}$	3.1	3.3	3.4	3.5	3.7	3.5	3.7	3.9	3.8	4.0	3.9	3.9	4.1	4.0	4.0
$J_{4'5'}$[c]	6.6	6.3	6.3	6.2	6.2	5.7	6.0	5.8	5.9	5.8	3.5	3.6	3.6	3.8	3.9
$J_{4'5''}$[c]	5.7	5.8	5.9	5.9	6.0	5.7	5.4	5.6	5.6	5.7	5.0	5.1	5.1	5.2	5.3

[a] Sample concentration = 15 mM. [b] Sample concentration = 2 mM. [c] Tentative assignment of H5′ and H5″, see text,[d], this number represents $J_{1'2'} + J_{1'2''}$. [e] This number represents $J_{2'3'} + J_{2''3'}$. [f] H2′ and H2″ almost coincide in the 500-MHz ^{1}H-NMR spectrum of thymidine at this temperature.

Table II. Conformational Features of **1**, **2**, and Thymidine in Solution: Time-Averaged Relative Distributions Over (i) Staggered Rotamers Around the C4′–C5′ Bond and (ii) North and South Conformers of the (Thio)furanose Ring[a]

	1	**2**	thymidine
$x(\gamma^+)$	0.30[b] (0.30)[c]	0.36[b] (0.36)[c]	0.49[d]
$x(\gamma^t)$	0.32[b] (0.38)[c]	0.28[b] (0.36)[c]	0.37[d]
$x(\gamma^-)$	0.38[b] (0.32)[c]	0.36[b] (0.28)[c]	0.14[d]
x(South)	0.72[e]	0.65[e]	0.67[f] (0.64)[g]
P(South), deg	177[e]	177	*h*
ν_m(South), deg	43[e]	44[e]	*h*
P(North), deg	13[e]	9[e]	*h*
ν_m(North), deg	45[e]	45[e]	*h*

[a] Sample temperature 300 K. [b] Refers to the assignment δ(H5′) > δ(H5″). [c] Refers to the assignment δ(H5′) < δ(H5″). [d] Assignment of H5′ and H5″ according to ref 11. [e] Obtained from PSEUROT analysis (see text). [f] Calculated from the equation *x*(South) = (16.9 − $J_{2'3'}$ − $J_{2''3'}$)/8.9 (ref 18). [g] Calculated from the equation *x*(South) = ($J_{1'2'}$ + $J_{1'2''}$ − 9.8)/5.9 (ref 18). [h] The pseudorotational parameters of the South or North conformers could not be derived (see text).

all this work is that small variations in the structure of a nucleoside analogue can produce drastic changes in its biological properties, such as toxicity or inhibitory action with respect to a particular enzyme (e.g., HIV reverse transcriptase or HSV-1 thymidine kinase). A currently common viewpoint is that the *conformational features of a particular nucleoside analogue* may be of decisive importance with respect to its biological activity.[2] X-ray crystallography has provided a wealth of structural information on nucleosides, nucleotides, and their analogues. Over 900 structures of this type have now been deposited in the Cambridge Crystallographic Data Base. It must be remembered, however, that most modified nucleosides are engaged in a conformational equilibrium in aqueous solution and (presumably) also under biological or physiological conditions.[3] It is for this reason that NMR spectroscopy can be a valuable complement to X-ray crystallographic studies; analysis of vicinal *J*-coupling constants and nuclear Overhauser effects can reveal important information about the *dynamic conformation in solution*, e.g. the equilibrium constant associated with conformational interchange, or the characteristics of the individual conformers can be derived.[4]

The viewpoint that an enzyme in action interacts with dynamic rather than static substrate molecules is far from new.[5] It is illustrative to distinguish two extreme cases with respect to the initial encounter of an enzyme and, say, a conformationally dynamic nucleoside analogue. One extreme is that the initial enzyme-modified nucleoside recognition is slow compared to the conformational interchange of the modified nucleoside. This means that all nucleoside conformations are exposed to the enzyme. The most reactive conformer will then be selected, even if its relative contribution to the conformational equilibrium is very small (Curtin–Hammett principle).[5] The other extreme is that the enzyme-modified nucleoside recognition is fast in comparison with the conformational interchange of the modified nucleoside. Then, the enzyme can distinguish between the different molecular conformers. An elegant example of the last extreme case is provided by the classic work of Belleau and Chevalier on the hydrolysis of conformationally constrained biphenyl systems by α-chymotripsin.[6]

In the present work, we report an integrated high field (500 MHz ^{1}H) NMR-X-ray crystallographic study on the conformation of 4′-thiothymidine (**1**) and (*E*)-5-(2-bromovinyl)-4′-thio-2′-deoxyuridine (**2**). The synthesis of these compounds was published earlier,[7] as well as an evaluation of their antiviral activity.[7a] Compound **1** was found to be toxic, whereas compound **2** is not

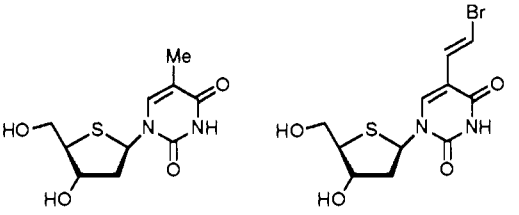

1 **2**

toxic and has substantial activity against some herpes viruses. The crystal structures of **1** and **2**, as well as their conformation in aqueous solution, are now described in detail. It is found that **1** and **2** adopt a conformation which closely resembles that of e.g. thymidine, i.e. substitution of O4′ by sulfur has only a minor influence on the molecular conformation. The results are discussed in terms of the stereoelectronic gauche effect and anomeric effect,[8] which are both expected to be less pronounced in **1** and **2**, in comparison with their natural (O4′) counterparts.

Results and Discussion

^{1}H NMR Studies on 1 and 2. Compounds **1** and **2** were studied in D_2O solution, at sample concentrations of 15 and 2 mM, respectively. Compound **2** is only marginally soluble in D_2O. One-dimensional ^{1}H NMR spectra were recorded at 500 MHz at the sample temperatures 285, 300, 313, 333, and 353 K. Table I compiles the vicinal proton–proton coupling constants ($^3J_{HH}$ values) abstracted from these spectra. The analogous data on unmodified thymidine are also given for comparison. The presence of sulfur instead of O4′ requires that some modifications be introduced in the routine procedures for characterizing the conformation of the C4′–C5′ bond and the 4′-thiofuranose ring. These

(2) (a) Taylor, E. W.; van Roey, P.; Schinazi, R. F.; Chu, C. K. *Antiviral Chem. Chemotherapy* **1990**, *1*, 163. (b) van Roey, P.; Salerno, J. M.; Chu, C. K.; Schinazi, R. F. *Proc. Natl. Acad. Sci. U.S.A.* **1989**, *86*, 3929 and references cited in these papers.

(3) Saenger, W., In *Principles of Nucleic Acid Structure*; Springer Verlag: New York, 1984.

(4) Neuhaus, D.; Williamson, M. In *The Nuclear Overhauser Effect in Structural and Conformational Analysis*; Verlag Chemie: Weinheim (FRG), 1989. (b) Davies, D. B. In *Progress in NMR Spectroscopy*; Pergamon Press Ltd.: Oxford, 1978; pp 135–225. (c) Altona, C. *Recl. Trav. Chim. Pays-Bas* **1982**, *101*, 413.

(5) See, for example: (a) Dugas, H., In *Bioorganic Chemistry. A Chemical Approach to Enzyme Action*, 2nd ed.; Springer Verlag: New York, 1988. (b) Eliel, E. L., In *Stereochemie der Kohlenstoffverbindungen*; Verlag Chemie: Weinheim, (FRG), 1966.

(6) Belleau, B.; Chevalier, R. *J. Am. Chem. Soc.* **1968**, *90*, 6864.

(7) (a) Dayson, M. R.; Coe, P. L.; Walker, R. T. *J. Med. Chem.* **1991**, *34*, 2782. (b) Uenishi, J.; Motoyama, M.; Nishiyama, Y.; Wakabayashi, S. *J. Chem. Soc., Chem. Commun.* **1991**, 1421. (c) Secrist, J. A., III; Tiwari, K. N.; Riordan, J. M.; Montgomery, J. A. *J. Med. Chem.* **1991**, *34*, 2361.

(8) (a) Kirby, A. J. In *The Anomeric Effect and Related Stereoelectronic Effects at Oxygen*; Springer Verlag: Berlin, 1983. (b) Deslongchamps, P. In *Stereoelectronic Effects in Organic Chemistry*; Pergamon Press: Oxford, 1983.

Scheme I

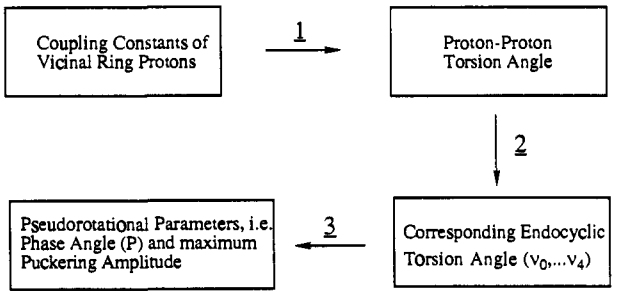

modifications will be discussed consecutively.

(a) Conformation of the C4′–C5′ Bond. This conformation was described in the usual terms, i.e. in terms of a rapid equilibrium over the staggered rotamers γ^+, γ^t, and γ^-.[9] The time-averaged relative populations of these rotamers ($x(\gamma^+)$, $x(\gamma^t)$, and $x(\gamma^-)$) could be solved from eqs 1a–c. The terms $J_{4'5'(5'')}{}^{\gamma(+)}$ etc. denote the *calculated* couplings between H4′ and H5′ (or H5″) in each

$$J_{4'5'(5'')}{}^{exp} = x(\gamma^+)J_{4'5'(5'')}{}^{\gamma(+)} + x(\gamma^t)J_{4'5'(5'')}{}^{\gamma(t)} + x(\gamma^-)J_{4'5'(5'')}{}^{\gamma(-)} \quad (1a,b)$$

$$x(\gamma^+) + x(\gamma^t) + x(\gamma^-) = 1 \quad (1c)$$

particular rotamer. We used the generalized Karplus equation, which contains corrections for electronegativity and orientation of substituents in 1,1,2-trisubstituted and 1,1,2,2,-tetrasubstituted ethane fragments.[9] This means that the presence of sulfur instead of O4′ was specifically accounted for. It is apparent from eqs 1a,b that a correct analysis of the C4′–C5′ conformation requires the assignment of H5′ and H5″ in the NMR spectrum.[4c,11] This is however not trivial in the case of **1** and **2**. For this reason, we have calculated $x(\gamma^+)$, $x(\gamma^t)$, and $x(\gamma^-)$ for both possible assignments, i.e. $\delta(H5') > \delta(H5'')$ and $\delta(H5') < \delta(H5'')$ (see Table II). It turns out that the results are virtually independent of the H5′/H5″ assignment; the three rotamers have approximately equal populations. It is noteworthy that this result differs considerably from the C4′–C5′ analysis in e.g. natural thymidine for which $x(\gamma^+) \approx 0.49$, $x(\gamma^t) \approx 0.37$, and $x(\gamma^-) \approx 0.14$ (Table II). We envisage two explanations for this difference between **1**, **2**, and thymidine: (i) The C4′–C5′ conformation in thymidine is determined in part by the *gauche effect*[10] (i.e. *gauche* orientation of O5′ and O4′ is energetically favored). The *gauche effect* is much weaker for **1** and **2** since sulfur is less electronegative than oxygen. (ii) The preference for γ^+ in thymidine is partly due to C6—H6···O5′ attraction.[3] This effect is expected to be relatively unimportant for **1** and **2**, since O5′ and C6 are placed further as a consequence of longer C–S bonds compared to C–O bonds.

(b) Conformation of the 4′-Thiofuranose Ring. The conformation of this ring was analyzed on the basis of the vicinal *J*-couplings $^3J_{1'2'}$, $^3J_{1'2''}$, $^3J_{2'3'}$, $^3J_{2''3'}$, and $^3J_{3'4'}$. We attempted to describe the experimental data in terms of a two-state equilibrium between a North-type puckered ring (phase angle $P \approx 0°$) and a South-type puckered ring ($P \approx 180°$), as is normally done for ribose or 2′-deoxyribose rings.[12] Such an analysis depends on three essential translational steps, as drawn schematically in Scheme I. In principle, the program PSEUROT incorporates all these translations for conformational analysis of nucleosides and nucleotides.[13] In the present case, we have carefully adapted the parametrization of PSEUROT in order to account for the presence of sulfur instead of O4′.

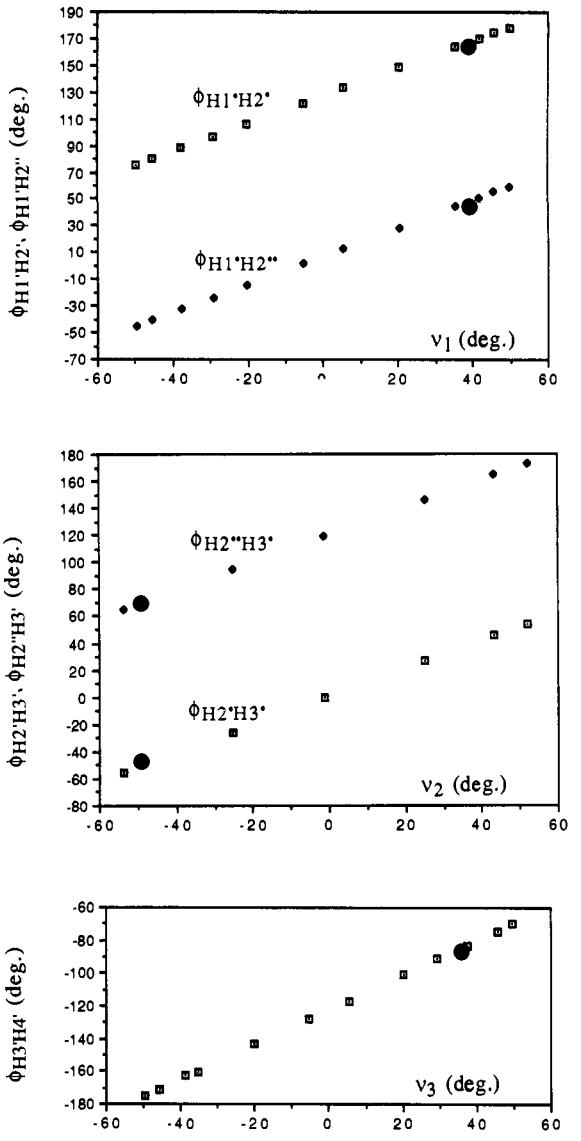

Figure 1. Calculated dependency of the proton–proton torsion angles $\phi_{H1'H2''}$, $\phi_{H1'H2''}$, $\phi_{H2'H3'}$, $\phi_{H2''H3'}$, and $\phi_{H3'H4'}$ on the corresponding endocyclic torsion angles (ν_1–ν_3) on the pseudorotational itineary. These points were abstracted from 12 ab initio MO calculations on structure **3** (HF/3-21G level). This set of calculations was carried out by fixing the torsions ν_0 and ν_4 in such a way that the puckering amplitude in all starting structures was 50°, while the phase angle of pseudorotation was incremented in 30° steps from 0° to 330°. The equations of the least-squares best-fit straight lines through the points are summarized in the text. The experimentally observed combinations of ϕ_{HH} and corresponding endocyclic torsion angles (shown as filled dots) are in agreement with the calculational results.

Translational step 1 (Scheme I) is covered by the generalized Karplus equation (vide supra); the substitution of O4′ by sulfur is readily incorporated. Translation step 2 is normally formulated as a set of linear equations of the form $\phi_{HH} = A\nu_j + B$.[14] Herein, ϕ_{HH} is the torsion angle between two vicinal ring protons and ν_j is the corresponding endocyclic torsion angle. The ν_j nomenclature is outlined below.[3] Note that each pair of vicinal ring protons has its own parameters *A* and *B*. The *A*,*B* sets for natural nucleosides and deoxynucleosides have been abstracted from a statistical survey of a set of crystal structures of nucleosides and

(9) (a) Haasnoot, C. A. G.; de Leeuw, F. A. A. M.; Altona, C. *Tetrahedron* **1980**, *36*, 2783. (b) Haasnoot, C. A. G.; de Leeuw, F. A. A. M.; Altona, C. *Org. Magn. Reson.* **1981**, *15*, 43. Application of the generalized Karplus equation to the C4′–C5′ bond in **1** and **2** yields the following: γ^+ rotamer, $J_{4'5'} = J_{4'5''} = 1.9$ Hz; γ^t rotamer, $J_{4'5'} = 4.1$ Hz, $J_{4'5''} = 11.5$ Hz; γ^- rotamer, $J_{4'5'} = 11.5$ Hz, $J_{4'5''} = 4.1$ Hz. It is assumed that the proton–proton torsion angles across the C4′–C5′ bond in the three rotamers, and are either 60°, −60°, or 180°.

(10) (a) Brunck, T. K.; Weinhold, F. *J. Am. Chem. Soc.* **1979**, *101*, 1700. (b) Olson, W. K. *J. Am. Chem. Soc.* **1982**, *104*, 278. (c) Wolfe, S. *Acc. Chem. Res.* **1972**, *5*, 102.

(11) Remin, M.; Shugar, D. *Biochem. Biophys. Res. Commun.* **1972**, *48*, 636.

(12) (a) Altona, C.; Sundalaringam, M. *J. Am. Chem. Soc.* **1972**, *94*, 8205; **1973**, *95*, 2333.

(13) (a) de Leeuw, F. A. A. M.; Altona, C. *J. Comput. Chem.* **1983**, *4*, 438. (b) de Leeuw, F. A. A. M.; Altona, C. QCPE, Program No. 463.

(14) de Leeuw, H. P. M.; Haasnoot, C. A. G.; Altona, C. *Isr. J. Chem.* **1980**, *20*, 108.

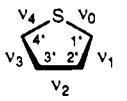

ν_0 = [C4′–S–C1′–C2′]
ν_1 = [S–C1′–C2′–C3′]
ν_2 = [C1′–C2′–C3′–C4′]
ν_3 = [C2′–C3′–C4′–S]
ν_4 = [C3′–C4′–S–C1′]

nucleotides.[14] It was found that *A* and *B* may differ considerably from their "standard" values, i.e. 1.000 for *A*, and −120°, 0°, or 120° for *B*. This is readily seen if one realizes that C1′, C2′, C3′, and C4′ in ribofuranose type structures are distorted from the perfect tetragonal geometry. We have attempted to derive the constants *A* and *B* for 4′-thiofuranose rings on the basis of a set of 12 ab initio MO calculations (HF/3-21G level)[15] on structure **3**. A puckering amplitude (ν_m) of 50° was chosen, and the phase

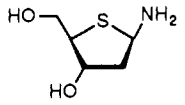

3

angle of pseudorotation (*P*) was incremented in 30°-steps from 0° to 330° by fixing torsion angles ν_0 and ν_4 during the optimizations. The five proton–proton torsion angles $\phi_{1'2'}$, $\phi_{1'2''}$, $\phi_{2'3'}$, $\phi_{2''3'}$, and $\phi_{3'4'}$ and the three corresponding endocyclic torsion angles ν_1, ν_2, and ν_3 were obtained from the resulting energy-optimized structures. The data are plotted in the graphs of Figure 1. The resulting linear equations are as follows: $\phi_{1'2'} = 127.3 + 1.0039\nu_1$, $\phi_{1'2''} = 7.2 + 1.0444\nu_1$, $\phi_{2'3'} = 0.2 + 1.0352\nu_2$, $\phi_{2''3'} = 120.32 + 1.0201\nu_2$, and $\phi_{3'4'} = -122.5 + 1.0594\nu_3$. Translation step 3 (Scheme I) poses a problem since the 4′-thiofuranose ring is not equilateral. Both C–S bonds are much longer than the three C–C bonds in the ring (ca. 1.83 Å for C–S and ca. 1.50 Å for C–C). Consequently, the classic pseudorotation concept (eq 2a)[12] does not provide a very accurate description of such rings. This problem has been recognized before and specifically solved for e.g. tetrahydrothiophene and 1,2-oxathiolane type rings.[16] It was found that eq 2a can best be extended by the parameters a_0, ..., a_4 and ϵ_0, ..., ϵ_4 (eq 2b).[16] *P* and ν_m have the same meaning in eqs 2a and 2b. Two additional ab initio MO calculations (HF/3-21G level) were performed on structure **3** in order to determine a_0, ...,

$$\nu_j = \nu_m \cos [P + 144°(j - 2)] \text{ with } j = 0, ..., 4 \quad (2a)$$

$$\nu_j = a_j\nu_m \cos [P + \epsilon_j + 144°(j - 2)] \text{ with } j = 0, ..., 4 \quad (2b)$$

a_4 and ϵ_0, ..., ϵ_4 in the 4′-thiofuranose ring. The starting structure for the first calculation had the 4′-thiofuranose ring in a North puckered conformation ($P = 0°$ and $\nu_m = 45°$), and the C4′–C5′ bond was rotated in the γ^t domain (γ(O5′–C5′–C4′–C3′) = 180°). The fully optimized geometry is shown as structure **4** in Figure 2. The starting structure for the second calculation was identical, except that the 4′-thiofuranose ring was placed in a South conformation ($P = 180°$ and $\nu_m = 45°$). The fully optimized structure is shown as **5** in Figure 2. The endocyclic torsion angles of the 4′-thiofuranose ring in **4** and **5** and the corresponding pseudorotational parameters are also given in Figure 2. It should be noted that the calculated geometry of the 4′-thiofuranose ring geometry in **5** closely resembles the experimental results as obtained via single-crystal X-ray diffraction on compounds **1** and **2** (vide infra). Parameters a_0, ..., a_4 and ϵ_0, ..., ϵ_4 could be solved directly from the calculated structures **4** and **5**, the results are compiled in Table III.[17] It was possible to test this parameter set on the basis of the crystal structures of compounds **1** and **2** (vide infra). The results of these tests are summarized in Table IV. These data show that application of eq 2a leads to appreciable differences

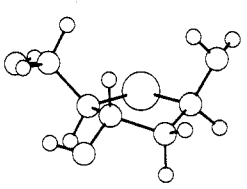

Structure **4**
$\nu_0 = 13.2°$, $\nu_1 = -38.0°$,
$\nu_2 = 52.1°$, $\nu_3 = -38.6°$,
$\nu_4 = 14.0°$.
$P = 0.5°$, $\nu_m = 49.0°$

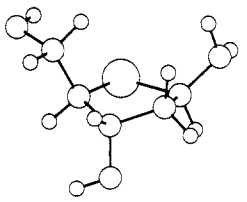

Structure **5**
$\nu_0 = -17.3°$, $\nu_1 = 41.6°$,
$\nu_2 = -53.7°$, $\nu_3 = 37.5°$,
$\nu_4 = -10.8°$.
$P = 176.1°$, $\nu_m = 50.6°$

Figure 2. Fully optimized geometries (ab initio HF/3-21G calculations) of **3**. Structure **4** (North conformation) was obtained using a starting geometry with $P = 0°$ and $\nu_m = 45°$, and structure **5** was obtained after starting from $P = 180°$ and $\nu_m = 45°$. These calculations were performed in three steps. First, a rough model was optimized with the semiempirical PM3 method, which however led to considerable flattening of the thiofuranose ring. Secondly, the bond lengths and bond angles from the PM3-optimized structure were used in the setup of the starting geometry for the ab initio calculations; bond lengths and bond angles were then optimized (HF/3-21G basis set) with all torsion angles constrained. Thirdly, the structure was fully optimized, using bond lengths and angles are obtained in step **2** in the starting structure.

Table III. Parameters a_0, ..., a_4 and ϵ_0, ..., ϵ_4 (Eq 3b) for the 4′-Thiofuranose Ring As Determined from the ab Initio (3-21G) Optimized Structures **4** and **5**

parameter	value	parameter	value
a_0	0.9888	ϵ_0	1.7
a_1	0.9952	ϵ_1	2.3
a_2	1.0645	ϵ_2	1.1
a_3	0.9792	ϵ_3	1.0
a_4	0.9859	ϵ_4	1.6

Table IV. Endocyclic Torsion Angles (deg) for the 4′-Thiofuranose Ring in Compounds **1** and **2**[a]

		torsions		torsions, parameters of Table III	
torsion	exptl (X-ray)	calcd (eq 2a)	diff[b]	calcd (eq 2b)	diff[b]
	Structure **1**				
ν_0 (C4′–S–C1′–C2′)	−14.5(2)	−16.6	2.1	−15.1	0.6
ν_1 (S–C1′–C2′–C3′)	39.0(3)	39.9	0.9	38.6	0.4
ν_2 (C1′–C2′–C3′–C4′)	−50.4(3)	−47.9	2.5	−50.9	0.5
ν_3 (C2′–C3′–C4′–S)	37.9(3)	37.6	0.3	36.3	1.6
ν_4 (C3′–C4′–S–C1′)	−13.0(3)	−13.0	0.0	−11.5	1.5
rms error			1.5		1.1
	Structure **2**				
ν_0 (C4′–S–C1′–C2′)	−12.9(3)	−15.4	2.5	−13.9	1.0
ν_1 (S–C1′–C2′–C3′)	37.9(4)	39.6	1.7	38.2	0.3
ν_2 (C1′–C2′–C3′–C4′)	−50.5(5)	−48.6	1.9	−51.7	1.2
ν_3 (C2′–C3′–C4′–S)	38.7(5)	39.1	0.4	38.6	0.1
ν_4 (C3′–C4′–S–C1′)	−14.3(9)	−14.6	0.3	−13.7	0.6
rms error			1.6		0.8

[a] Calculated values for ν_0 ..., ν_4 according to eq 2a and eq 2b are compared with the crystal structural data. See text. [b] Absolute value of the difference between the calculated and experimental torsion angle.

(15) Gaussian 90, Revision H: Frisch, M. J.; Head-Gordon, M.; Trucks, G. W.; Foresman, J. B.; Schlegel, H. B.; Raghavachari, K.; Robb, M.; Binkley, J. S.; Gonzalez, C.; Defrees, D. J.; Fox, D. J.; Whiteside, R. A.; Seeger, R.; Melius, C. F.; Baker, J.; Martin, R. L.; Kahn, L. R.; Stewart, J. J. P.; Topiol, S.; Pople, J. A., Gaussian, Inc.: Pittsburg PA, 1990.

(16) (a) de Leeuw, F. A. A. M.; van Kampen, P. N.; Altona, C.; Diez, E.; Esteban, A. L. *J. Mol. Struct.* **1984**, *125*, 67. (b) See also: Haasnoot, C. A. G.; Liskamp, R. M. J.; van Dael, P. A. W.; Noordik, J. H.; Ottenheim, H. C. J. *J. Am. Chem. Soc.* **1983**, *105*, 5406.

(17) Our method for solving this will be shown for a_2 and ϵ_2. Equations 3a,b are obtained from structures **4** and **5**, respectively:

$$\nu_2 = 52.2 = 49.0a_2 \cos (0.5 + \epsilon_2) \quad (3a)$$

$$\nu_2 = -53.7 = 50.6a_2 \cos (176.1 + \epsilon_2) \quad (3b)$$

Combination gives: $a_2 = 1.0645$ and $\epsilon_2 = -1.1°$. The remaining parameters *a* and ϵ were solved analogously.

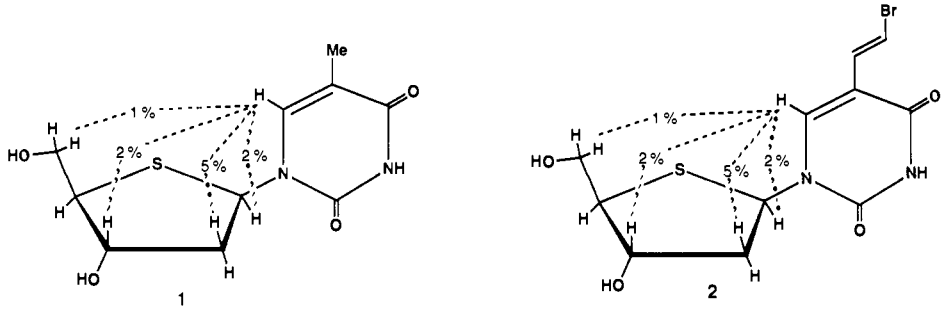

Figure 3. NOe enhancements as obtained upon irradiation of H6 in compounds **1** and **2**. The clear nOe contact between H6 and H2′ indicates predominant anti orientation of the base, in both **1** and **2** (see text).

between the calculated and observed endocyclic torsion angles. The largest difference (2.5°) is found for the torsion around the C2′–C3′ (ν_2) and S–C1′(ν_0), and the overall root-mean-square error is 1.5–1.6°. Refinement of the pseudorotation equation through use of eq 2b and a_0, ..., a_4 and ϵ_0, ..., ϵ_4 from Table III leads to an improved description of the 4′-thiofuranose ring. The largest difference is then 1.0–1.6°, and the overall root-mean-square error drops to 0.8–1.1° (Table IV).

Running PSEUROT based on the experimental *J*-couplings in Table I and the parametrizations as discussed above revealed that the 4′-thiofuranose ring in **1** and **2** has a preference for a South-type puckered conformation in solution. The preferred conformations for **1** and **2** have almost identical pseudorotational parameters (**1**: P = 177°, ν_m = 43°; **2**: P = 177°, ν_m = 44°). The population of the South form (x(South)) is slightly larger for **1** than for **2** and decreases with increasing sample temperature (**1**: x(South) = 75% at 285 K and 67% at 353 K; **2**: x(South) = 67% at 285 K and 63% at 353 K). Interestingly, the PSEUROT analysis also provides information about the minor North-type conformer. Its pseudorotation parameters are as follows: P = 13°, ν_m = 45° for **1** and P = 9°, ν_m = 45° for **2**. This means that the minor conformer assumes a standard North-type conformation, ranging between the canonical C3′-endo/C2′-exo twist and C3′-endo envelope structures. It should be realized that the North-type conformer has an appreciable contribution to the conformational equilibrium, i.e. its relevance with respect to biological activity cannot be neglected a priori. Furthermore, we wish to emphasize that characterization of the minor conformer is a typical advantage of NMR conformational analysis; the conformation of the major South puckered participant in the conformational blend closely resembles the X-ray structure (vide infra). With respect to the quality of the PSEUROT fit, it is important to note that the differences between calculated and experimentally observed *J*-coupling constants were very small in both cases. The largest individual difference between calculated and experimental *J*-coupling for **1** amounts to 0.21 Hz and the overall root-mean-square error was 0.14 Hz. For **2**, these numbers are 0.29 Hz and 0.12 Hz, respectively.

For comparison, we also examined the conformation of the furanose ring in unmodified thymidine.[29] At 300 K, it is found that x(South) ≈ 67% (Table I), i.e., the distribution over North and South is virtually the same for **1**, **2**, and thymidine. It was not possible, however, to obtain the phase angle and puckering amplitude of the South and North conformers of thymidine, since (i) the full set of *J*-couplings ($J_{1'2'}$, $J_{1'2''}$, $J_{2'3'}$, $J_{2''3'}$, and $J_{3'4'}$) could only be determined at two temperatures (333 and 353 K, see Table I) and (ii) the North–South conformational equilibrium does not change upon going from 333 to 353 K. This means that there are merely five experimental input values available for the PSEUROT procedure, while five conformational parameters are requested also (i.e., P(South), ν_m(South), P(North), ν_m(North), and x(South)). Under these circumstances, the outcome of PSEUROT is quite sensitive to experimental inaccuracies.[13,29] For this reason, we have restricted ourselves to the use of the formulas x(South) = $(16.9 - J_{2'3'} - J_{2''3'})/9.9$ and x(South) = $(J_{1'2'} + J_{1'2''} - 9.8)/5.9$, as proposed by Rinkel and Altona.[18]

(18) Rinkel, L. J.; Altona, C. *J. Biomol. Struct. Dyn.* **1987**, *4*, 621.

We also performed NMR experiments to determine the preferred conformation around the glycosidic (C1′–N1) bond, i.e. anti or syn orientation of the base. Figure 3 schematically shows the observed nOe enhancements that were observed for H1′, H2′, H3′, and H5′/5″, upon specific irradiation of H6. For both compounds, the largest nOe enhancement is found for the H2′ resonance (5%), which clearly indicates predominant anti orientation of the base.[4,19] This result is not surprising, since pyrimidine bases generally have a pronounced preference for anti conformation around the glycosidic bond.[3] Moreover, anti conformation of the base is also found in the crystal structures of **1** and **2** (vide infra).

An alternative approach to determine the glcosidic conformation is based on measurement of the vicinal $^3J_{H1'C2}$ and $^3J_{H1'C6}$ coupling constants.[4b,20] According to Davies[4b] and Lemieux et al.,[20] the Karplus equation $^3J_{HC} = 6.7 \cos^2 \phi - 1.3 \cos \phi$ can be used; ϕ is the torsion angle [H1′–C1′–N1–C2(6)]. From the INEPT ^{13}C spectrum of **1**, we obtained $^3J_{H1'C2} \approx 3$ Hz and $^3J_{H1'C6} \approx 2$ Hz, which leads to four approximate solutions for ϕ in each case.[7c] The calculated approximate values for $\phi_{H1'C2}$ are 40°, −40°, 125°, and −125°, and the corresponding values for the glycosidic torsion angle χ[O4′–C1′–N1–C2] are (in increasing order) 80°, 160°, 245°, and 355°. Similarly, the calculated approximate values for $\phi_{H1'C6}$ are 50°, −50°, 115°, and −155°, which leads to the glycosidic torsion angles (in increasing order) 55°, 185°, 250°, and 350°. It must be concluded that this analysis does not provide a consistent picture of the glycosidic conformation in **1**. We envisage two possible explanations for these findings: (i) the presence of sulfur instead of O4′ may influence the spin–spin coupling between H1′ and C2/C6, i.e. the Lemieux equation is then no longer reliable; (ii) a conformational equilibrium, either between a syn and an anti conformation, or equilibration within the anti domain, can complicate the application of the Lemieux procedure. We conclude that measurement of nOe contacts (vide supra) is the method of choice in order to characterize the glycosidic conformation in **1** and **2**.

Crystal Structures of 1 and 2. The crystal structures of compounds **1** and **2** are shown in Figures 4 and 5. Table V summarizes the most important conformational characteristics for the two structures **1** and **2**. Atomic coordinates, positional parameters, crystal parameters, and information concerning intensity measurements and solution/refinement are provided in the supplementary material. The 4′-thiofuranose ring of **1** is found in a South-type puckered conformation with pseudorotation phase angle P = 177.7 (4)° and maximum puckering amplitude ν_m = 47.9 (4)°. The bond lengths C1′–S and C4′–S are 1.839 (3) and

(19) Rosemeyer, H.; Toth, G.; Golankiewicz, B.; Kazimierczuk, Z.; Bourgeois, W.; Kretschmer, U.; Muth, H.-P.; Seela, F. *J. Org. Chem.* **1990**, *55*, 5784.

(20) (a) Lemieux, R. U.; Nagabhushan, T. L.; Paul, B. *Can. J. Chem.* **1972**, *50*, 773. (b) Delbaere, L. T. J.; James, M. N. G.; Lemieux, R. U. *J. Am. Chem. Soc.* **1973**, *95*, 7866. (c) Davies, D. B. In *Progress in NMR Spectroscopy*; Pergamon Press, Ltd.: London, 1987; Vol. 12, pp 135–225. (d) Davies, D. B.; Rajani, P.; Sadikot, H. *J. Chem. Soc., Perkin Trans. II* **1985**, 279. (e) Davies, D. B.; Rajani, P.; MacCoss, M.; Danyluk, S. S. *Magn. Res. Chem.* **1985**, *23*, 72.

(21) Other coupling constants that could be deduced from this particular region in the INEPT spectrum of **1** are the following: $^3J_{H6C2} \approx 8$ Hz, $^1J_{H6C6} \approx 187$ Hz, and $^3J_{Me(H)C6} \approx 6$ Hz.

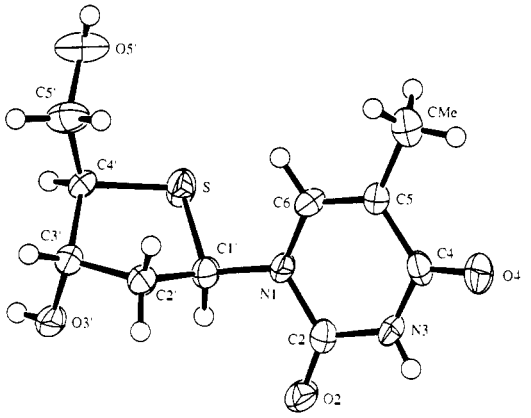

Figure 4. ORTEP drawing of the crystal structure of compound **1**. The most important conformational features (trans conformation around C4'–C5', South conformation of the 4'-thiofuranose ring, anti orientation of the base) are clearly visible.

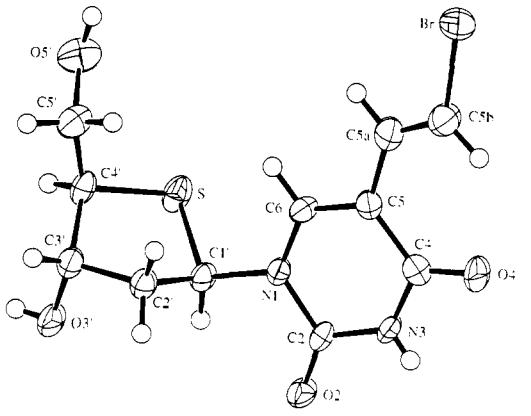

Figure 5. ORTEP drawing of the crystal structure of compound **2**. Note the close similarity between the crystal structures of **1** and **2**.

1.831 (3) Å, respectively, while the bond lengths C1'–C2', C2'–C3', and C3'–C4' are 1.525 (4), 1.508 (4), and 1.545 (4) Å, respectively. These data clearly illustrate the nonequilateral nature of the five-membered ring in **1** (vide supra). The C4'–C5' (γ) bond in **1** is found in the γ(trans) conformation with γ[O5'–C5'–C4'–C3'] = 179.0 (2)°. The glycosidic bond length N1–C1' and bond angle N1–C1'–S are 1.480 (4) Å and 113.5 (2)°, respectively. The thymine base is in the anti conformation with glycosidic torsion χ[C2–N1–C1'–S] = −144.2 (3)°. The thymine moiety has the usual geometry; the mean deviation of all non-hydrogen atoms of thymine from the least-squares plane is only 0.0129 Å. Molecules in the crystal structure of **1** are linked in a three-dimensional lattice through three independent intermolecular hydrogen bonds. The distance and angle data are as follows (no esd's for the angle involving hydrogen and the O–H distance since H is not refined): (i) H bond O5'···H–O5', angle = 148°, d[H–O5'] = 1.93 Å, d[O5'–O5'] = 2.771 (1) Å; (ii) H bond O4···H–O3', angle = 145°, d[H–O4] = 1.96 Å, d[O4–O3'] = 2.773 (3) Å; and (iii) H bond O3'···H–N3, angle = 166°, d[H–O3'] = 2.06 (4) Å, d[O3'–N3] = 2.996 (3) Å. The crystal structure of compound **2** is shown in Figure 5. Further information on the crystal structure of **2** is compiled in Table V. The 4'-thiofuranose ring in **2** also adopts a South-type puckered geometry. The phase angle of pseudorotation (P) equals 179.5°, and the puckering amplitude (ν_m) is 48.6°. The crystal structure of **2** also reveals the unequilateral nature of the five-membered ring: the bond lengths C1'–S and C4'–S are 1.842 (4) and 1.838 (4) Å, respectively, while the bonds C1'–C2', C2'–C3', and C3'–C4' are much shorter (i.e., 1.521 (6), 1.501 (6), and 1.539 (5) Å, respectively). The C4'–C5' conformation is γ^t, with γ = −174.0 (3)°. The glycosidic bond length and bond angle (vide supra) are 1.472 (5) Å and 112.7 (2)°, respectively. The modified uracil base is in the anti conformation with glycosidic torsion χ = −139.0 (3)°. These data

Table V. Geometric Parameters: Bond Lenghts, Angles, and Torsion Angles That Represent Important Structural Features of **1**, **2**, and Thymidine[a,23c]

	1	**2**	thymidine[23c]
Bond Lengths (Å) and Angles (deg)			
C1'–C2'	1.525 (4)	1.521 (6)	1.515 (7)
C2'–C3'	1.508 (4)	1.501 (6)	1.523 (7)
C3'–C4'	1.545 (4)	1.539 (5)	1.529 (7)
C1'–S[b]	1.839 (3)	1.842 (4)	1.434 (5)
C4'–S[b]	1.831 (3)	1.838 (4)	1.460 (5)
C1'–N1	1.480 (4)	1.472 (5)	1.480 (6)
C1'–C2'–C3'	106.2 (3)	107.1 (4)	102.7 (4)
C2'–C3'–C4'	106.6 (2)	106.6 (3)	102.1 (3)
C3'–C4'–S[b]	105.4 (2)	105.0 (2)	104.4 (3)
C4'–S–C1'[b]	94.0 (1)	94.1 (2)	110.1 (3)
S–C1'–C2'[b]	105.9 (2)	105.5 (2)	106.5 (3)
S–C1'–N1[b]	113.5 (2)	112.7 (2)	108.2 (4)
Torsion Angles (deg)			
C4'–S–C1'–C2'[b] (ν_0)	−14.5 (2)	−12.9 (3)	−7.0 (3)
S–C1'–C2'–C3'[b] (ν_1)	39.0 (3)	37.9 (4)	27.8 (3)
C1'–C2'–C3'–C4' (ν_2)	−50.4 (3)	−50.5 (5)	−36.9 (4)
C2'–C3'–C4'–S[b] (ν_3)	37.9 (3)	38.7 (5)	33.2 (4)
C3'–C4'–S–C1'[b] (ν_4)	−13.0 (3)	−14.3 (4)	−16.7 (4)
S–C1'–N1–C2[b] (χ)	−144.2 (3)	−139.0 (3)	−139.4 (3)
O5'–C5'–C4'–C3' (γ)	179.0 (2)	−174.0 (3)	165.3 (3)
Pseudorotation Parameters (deg)			
phase angle (P)	177.7	179.5	187.5
puckering amplitude (ν_m)	47.9	48.6	37.8

[a] Esds are given in parentheses. [b] S represents O4' in the case of thymidine.

show that there is a close similarity between the crystal structures of compounds **1** and **2**. Molecules in the crystal structure of **2** are also linked in a three-dimensional lattice through three independent intermolecular hydrogen bonds. The distance and angle data are as follows (no esd's for the angle involving hydrogen and the O–H distance since H is not refined): (i) H bond O5'···H–O5', angle = 141°, d[H–O5'] = 2.32 Å, d[O5'–O5'] = 3.117 (3) Å; (ii) H bond O4···H–O3', angle = 166°, d[H–O4] = 1.85 Å, d[O4–O3'] = 2.796 (4) Å; and (iii) H bond O3'···H–N3, angle = 160°, d[H–O3'] = 2.41 Å, d[O3'–N3] = 3.023 (4) Å. The intermolecular distances for the atoms involved in hydrogen bonding indicate that hydrogen bonding is stronger in the structure of **1** than in **2**.

Further information on both crystal structures, including pictures of the three-dimensional lattice of both structures, is provided in the supplementary material.

Concluding Remarks

The conformational properties of **1** and **2** in solution and in the crystalline state show a quite consistent picture. The predominant conformation in solution can be characterized in shorthand as follows: South (thiofuranose ring), anti (base orientation). The conformation in the solid state is analogous. The NMR data indicate that a second conformation with a North-type puckered thiofuranose ring is present in solution. In principle, such a minor conformer can be responsible for biological activity, i.e. the best basis for formulating structure–activity relationships for modified nucleosides is probably a combined interpretation of solid-state and solution conformational data. In our previous work,[22] we have argued that the conformational preference of the furanose ring

(22) (a) Koole, L. H.; Buck, H. M.; Nyilas, A.; Chattopadhyaya, J. *Can. J. Chem.* **1987**, *65*, 2089. (b) Koole, L. H.; Wu, J.-C.; Neidle, S.; Chattopadhyaya, J. *J. Am. Chem. Soc.* **1992**, *114*, 2687.

(23) (a) Watson, D. G.; Sutor, D. J.; Tollin, P. *Acta Crystallogr.* **1965**, *19*, 111. (b) Young, D. W.; Wilson, H. R. *Acta Crystallogr.* **1975**, *B31*, 961. (c) Young, D. W.; Tollin, P.; Wilson, H. R. *Acta Crystallogr.* **1969**, *B25*, 1423. (d) Gartland, G. L.; Bugg, C. E. *Acta Crystallogr.* **1977**, *B33*, 3678. (e) Lai, T. F.; Marsh, R. E. *Acta Crystallogr.* **1982**, *B28*, 1982. (f) Furberg, S.; Petersen, C. S.; Romming, Chr. *Acta Crystallogr.* **1965**, *18*, 313. (g) Green, E. A.; Rosenstein, R. D.; Shiono, R.; Abraham, D. J.; Trus, B. L.; Marsh, R. E. *Acta Crystallogr.* **1975**, *B31*, 102. (h) Thewalt, U.; Bugg, C. E.; Marsh, R. E. *Acta Crystallogr.* **1970**, *B26*, 1089.

in 2′-deoxynucleosides can in fact be regarded as an energetic balance between (i) the gauche effect,[10] which favors a South-type conformation since O4′ and O3′ then more or less achieve a gauche-type arrangement, and (ii) the anomeric effect,[8] which favors a North-type conformation, since the C1′–N1(9) bond is then antiperiplanar with respect to one of the lone pairs of O4′. Comparing compounds **1** and **2** with e.g. thymidine,[29] it must be expected that *both the gauche effect and the anomeric effect are weaker in 1 and 2 than in thymidine, since sulfur is less electronegative in comparison with oxygen.* The similarity of the North–South conformational equilibria[29] in **1**, **2**, and thymidine indicates that the *balance of the gauche and anomeric effect remains virtually unaffected by the substitution of O4′ by sulfur.*

Evidently, it is difficult to substantiate the theory that the anomeric effect in **1** and **2** is really small compared to that in naturally occurring nucleosides. A possible clue is provided via comparison of the bond lengths C1′–O4′(S) and C4′–O4′(S). For natural nucleosides it is generally found that C4′–O4′ is significantly longer than C1′–O4′. It has been advocated by Kirby that the reason for this difference is the anomeric effect.[8a] According to the simplified valence bond model description of the anomeric effect, the C1′–O4′ bond obtains a partial double-bond character and is therefore shortened. In the case of **1** and **2**, we have found that C1′–S and C4′–S are *virtually equally long* which may support the idea of a weaker anomeric effect. It should also be noted, however, that the findings of de Leeuw et al.[14] that no clear correlations of variation of C1′–O4′ bond lengths with either χ or ϕ(C4′–O4′–C1′–N) was obtained contradict that the anomeric effect is responsible for the shortening of C1′–O4′ with respect to C4′–O4′ in natural (O4′) nucleosides and nucleotides.

Experimental Section

NMR Spectroscopy. ^{1}H NMR spectra were recorded at 500.13 MHz on a Bruker AMX 500 system. D_2O (99.8+% deuterium) was used as the solvent. The sample temperature was controlled within a range of approximately 0.2 centigrades. Sample concentrations were approximately 15 mM for **1** and 2 mM for **2**. All measurements were performed under identical spectral and processing conditions: 5000 Hz sweep width, 32K time domain, zero-filling to 64K, and slight apodization (resolution enhancement with line broadening of −1 Hz). Virtually all subspectra were found to be first order, which facilitated extraction of *J*-coupling constants and chemical shifts. Some spectral patterns were simulated with a standard computer simulation algorithm. One-dimensional nOe experiments were run with 2 s of irradiation time and a decoupling power of 50 dB below 0.2 W. NOe difference spectra were obtained upon subtraction of on- and off-resonance spectra after identical line broadening (0.25 Hz exponential multiplication) and Fourier transformation.

X-ray Diffraction and Structure Determination of 1 and 2. Colorless, needle-shaped single crystals of **1** and **2** were obtained after recrystallization from ethanol (for **1**) or a methanol/ethanol mixture (for **2**). The dimensions of the crystals used for X-ray diffraction are approximately 0.450 × 0.200 × 0.030 mm for **1** and 0.600 × 0.080 × 0.050 mm for **2**. All measurements were made on a Rigaku AFC5R diffractometer with graphite monochromated Cu Kα radiation and a 12 KW rotating anode generator. Cell constants and an orientation matrix for data collection, obtained from a least-squares refinement using the setting angles of 21 ($40.5 < 2\theta < 58.9°$) and 25 ($79.3 < 2\theta < 80.1°$) carefully centered reflections (for **1** and **2** respectively) corresponded to monoclinic cells in both cases. The cell dimensions are the following: a = 9.2389 (9) Å, b = 5.1796 (9) Å, c = 12.0840 (8) Å, β = 93.125 (6)°, V = 575.4 (1) Å^3 for **1**, and a = 9.424 (2) Å, b = 5.260 (2) Å, c = 12.762 (1) Å, β = 91.72 (1)°, V = 632.3 (2) Å^3 for **2**.

Based on the systematic absence of $0k0$ ($k \neq 2n + 1$), packing considerations, a statistical analysis of intensity distribution, knowledge of enantiomeric purity of the compounds, and the successful solution and refinement of the structure, the space group was determined to be $P2_1$ (No. 4) in both cases.

The data were collected at a temperature of 23 ± 1 °C using the ω–2θ scan technique to a maximum 2θ value of 120°. ω scans of several intense reflections, made prior to data collection, had an average width at half-height of 0.24° for **1** and 0.39° for **2**. The take-off angle was 6.0° in both cases. Scans of $(1.42 + 0.14 \tan \theta)°$ for **1** and $(1.52 + 0.14 \tan \theta)°$ for **2** were made at a speed of 16.0 deg/min (in ω). The weak reflections ($I < 20.0\sigma(I)$) were re-scanned up to 3 times to ensure good counting statistics. Stationary background counts were recorded on each side of the reflection. The ratio of peak counting time to background counting time was 2:1.

For **1**, 2049 reflections were collected, of which 937 were unique (R_{int} = 0.029). For **2**, 2262 reflections were collected, 1061 of which were unique (R_{int} = 0.026). Three standards were monitored after every 150 reflections. The standards varied in a nonsystematic manner, with less than 4% overall change. The linear absorption coefficient, μ, is 25.8 cm^{-1} for **1** and 61.2 cm^{-1} for **2**. An emperical ψ-scan absorption correction was applied to both structures. Further details concerning data reduction are provided in the supplementary material.

Structure **1** was solved by direct methods,[24a] and structure **2** was solved by the Patterson heavy-atom method.[24b] The non-hydrogen atoms were refined anisotropically. All hydrogen atoms were located from difference Fourier syntheses included in the structure factor calculation in idealized positions and were assigned to isotropic thermal parameters which were 20% greater than the B_{eq} value of the atom to which they were bonded. The absolute configurations were confirmed using Bijvoet reflections. The final cycle of full-matrix least-squares refinement was based on 943 observed reflections ($I > 3\sigma(I)$) and 153 variables for **1**. For **2**, these numbers are 1027 observed reflections and 171 variables. The unweighted and weighted agreement factors were

$$R = \sum||F_o| - |F_c||/\sum|F_o| = 0.029 \text{ for } \mathbf{1} \text{ and } 0.022 \text{ for } \mathbf{2}$$

$$R_w = [(\sum(|F_o| - |F_c|)^2/\sum wF_o^2)]^{1/2} = 0.029 \text{ for } \mathbf{1} \text{ and } 0.024 \text{ for } \mathbf{2}$$

The standard deviation of an observation of unit weight was 3.17 for **1** and 2.10 for **2**. The weighting scheme was based on counting statistics and included in a *p*-factor of 0.01 for structure **2** to downweight the intense reflections. The final difference Fourier maps were featureless, with maximum and minimum peaks in the range ±0.19 and ±0.24 e/Å^3 for **1** and **2**, respectively. Neutral atom scattering factors were taken from Cromer and Waber.[25] Anomalous dispersion effects were included in F_{calc};[26] the values for $\Delta f'$ and $\Delta f''$ were those of Creagh and McAuley.[27] All calculations were performed using the teXsan[28] crystallographic software package of Molecular Structure Corp.

Acknowledgment. We thank the Swedish Board for Technical Development and Swedish Natural Science Research Council,

(24) (a) Sheldrick, G. M. The SHELXS-86 crystallographic program for the solution of crystal structures. Institut für Anorganische Chemie der Universität Göttingen, Taumanstrasse 4, Göttingen, Germany, 1986. (b) Calbrese, J. C. PHASE—Patterson Heavy Atom Solution Extraction, University of Wisconsin–Madison, Ph.D. Thesis, 1972.

(25) Cromer, D. T.; Waber, J. T. In *International Tables for X-ray Crystallography*; The Kynoch Press: Birmingham, England, 1974.

(26) Ibers, J. A.; Hamilton, W. C. *Acta Crystallogr.* **1964**, *17*, 781.

(27) Creagh, D. C.; McAuley, W. J. *International Tables for Crystallography*; Wilson, A. J. C., Ed.; Kluwer Academic Publishers: Boston, 1992; Vol. C, Table 4.2.4.3, pp 200–206.

(28) teXsan: Crystal Structure Analysis Package, Molecular Structure Corporation, 3200 Research Forest Drive, The Woodlands, TX 77381 (1985 and 1992).

(29) It was suggested[9b,12b] that the population of the North and South conformers of 2′-deoxyadenosine and other 2′-deoxynucleosides in D_2O solution changes only slightly with temperature (75% S at 18 °C and 73% S at 60 °C). This led these workers to assume (see ref 49)[12b] that the enthalpy ($\Delta H°$) difference between North and South puckered sugar in 2′-deoxynucleosides is close to zero and subsequently they back-calculated [$R \ln K = \Delta S° \approx$ constant for $\Delta H° = 0$] to match equilibrium N and S population with assumed "reasonable $\Delta S°$ values".[9b,12b] Our unpublished experimental results from 500-MHz ^{1}H-NMR analysis, however, show that the equilibrium population of N and S conformers does change *noticeably* within a **larger** temperature range: thus for 2′-dA (76% S at 5 °C and 68% S at 85 °C) P_S = 164° and ν_m = 35°, for 2′-dG (72% S at 5 °C and 66% S at 85 °C) P_S = 165° and ν_m = 33°, and for 2′-dC (66% S at 5 °C and 63% S at 85 °C) P_S = 154° and ν_m = 34° [Note: P_N = 10° and ν_m = 35° are constrained[9b]]. Simple van't Hoff plots ([$\ln (X_S/X_N)$] versus $1/T$ at five different temperatures from 5 to 85 °C) show $\Delta H°$ and $\Delta S°$ of the conformational equilibria: $\Delta H°$ = −4.7 kJ/mol and $\Delta S°$ = −6.7 J/(mol K) for 2′-dA; $\Delta H°$ = −2.8 kJ/mol and $\Delta S°$ = −1.6 J/(mol K) for 2′-dG; $\Delta H°$ = −1.3 kJ/mol and $\Delta S°$ = +1.3 J/(mol K) for 2′-dC. Note that the pseudorotational analyses of conformational behavior of thymidine were impossible to determine accurately by ^{1}H NMR owing to the fact that H2′ and H2″ are near-isochronous.[18] The temperature dependence studies of North–South equilibrium in **1** gave $\Delta H°$ = −5.0 kJ/mol and $\Delta S°$ = −7.5 J/(mol K), while the corresponding values for **2** are −2.5 kJ/mol and −1.7 J/(mol K). The error limits of all $\Delta H°$ and $\Delta S°$ values are ±0.8 kJ/mol and ±3.3 J/(mol K), respectively. It is thus clear from the experimental data that at room temperature (25 °C) the $\Delta H°$ and $T\Delta S°$ contributions to $\Delta G°$ are at least comparable in 2′-dA, 2′-dG, 2′-dC, **1** and **2**. In conclusion, our experimental data suggest that it is the fine balance of gauche and anomeric effects ($\Delta H°$) that has significant contributions for driving the North–South equilibria in 3′-deoxynucleosides and 2′- or 3′-amino-substituted nucleosides, and 2′-deoxynucleosides are not certainly any exception.

Swedish Board for Technical Development (NUTEK) and Medivir AB, Lunastigen 7, S-141 44 Huddinge, Sweden, for generous financial support (to J.C.). Thanks are due to the Wallenbergstiftelsen, Forskningsrådsnämnden, and University of Uppsala for funds for the purchase of a 500-MHz Bruker AMX NMR spectrometer in J.C.'s lab. The Science and Engineering Research Council and the Wellcome Foundation Ltd. are gratefully acknowledged for generous financial support (to R.T.W.). Financial Support from the European Molecular Biology Organization (EMBO) through a 2-year EMBO fellowship to L.H.K. is gratefully acknowledged.

Supplementary Material Available: Experimental details and tables of atomic coordinates, positional atomic coordinates, thermal parameters, bond distances, bond angles, torsion angles, intermolecular contacts, least-squares planes, and intensity data (24 pages); listing of structure factors (8 pages). Ordering information is given on any current masthead page.

Self-Assembled Monolayers of Parent and Derivatized [n]Staffane-3,3$^{(n-1)}$-dithiols on Polycrystalline Gold Electrodes

Yaw S. Obeng,[†] Mark E. Laing,[‡] Andrienne C. Friedli, Huey C. Yang, Dongni Wang,[§] Erik W. Thulstrup,[∥] Allen J. Bard,* and Josef Michl*,[⊥]

Contribution from the Department of Chemistry and Biochemistry, The University of Texas at Austin, Austin, Texas 78712-1167. *Received April 2, 1992*

Abstract: Synthesis of the terminally disubstituted rigid rod molecules, [n]staffane-3,3$^{(n-1)}$-dithiols, n = 1-4, and their singly functionalized derivatives carrying an acetyl or a pentaammineruthenium(II), $[Ru(NH_3)_5]^{2+}$, substituent is described. Self-assembled monolayers of the neat [n]staffane derivatives and of their mixtures with n-alkyl thiols were prepared on polycrystalline gold electrodes. Grazing incidence FTIR spectroscopy and comparison with polarized IR spectra of model compounds oriented in stretched polyethylene revealed that, in the films assembled directly from the dithiols, the average orientation of the [n]staffane rods was halfway between perpendicular and parallel to the surface, whereas, in the films obtained from the singly functionalized derivatives, the rods were nearly perpendicular to the surface. The degree of ordering and packing was also investigated by contact angle measurements with deionized water. The electrode blocking properties of the films were investigated by three independent electrochemical techniques, cyclic voltammetry in a solution containing $K_4Fe(CN)_6$, chronoamperometry in a solution of $Ru(NH_3)_6Cl_3$, and cyclic voltammetry of the gold surface in sulfuric acid. The results from the three methods were in good agreement and showed that the films assembled from the dithiols were not as well organized as those obtained from the monoderivatized analogues. In situ hydrolytic removal of the protective acetyl groups and subsequent functionalization of the resultant film covered with free thiol groups with aquapentaammineruthenium(II), $[Ru(NH_3)_5(H_2O)]^{2+}$, are possible without disturbing the structure of the film. Electrodes covered with monolayers carrying ruthenium pentaammine groups on their outer surface exhibit oxidation-reduction waves at 0.51 V vs SCE attributable to the Ru(II)-Ru(III) couple, demonstrating electron transfer across the monolayer. The formal potential of the immobilized couple is about 60-mV more positive than that of the dissolved complex, $[[(NH_3)_5Ru]$-[n]staffanedithiol$]^{2+}$, in 1 M $HClO_4$ solution. The surface concentration of Ru is the same in the films assembled from this complex and those produced by in situ functionalization of a film covered with free thiol groups and corresponds to a monolayer of $(NH_3)_5Ru$. However, in the former type of film, the surface concentration of the staffane rods is only about half of that in the latter, implying that only about half of the surface thiol groups have been metalated.

Introduction

Terminally disubstituted [n]staffanes ([**n**]**1**) were originally developed for use as assembly elements in a molecular-size "Tinkertoy" construction set[1-4] but can also be viewed simply as a new class of straight and fairly rigid inert spacers suitable for investigations of electron and energy transfer. In this regard, terminal disubstitution with thiol-based groups[3-5] is particularly interesting, and preliminary results of an optical investigation of intramolecular electron transfer between Ru(II) and Ru(III) attached to 3,3$^{(n-1)}$-bis(methylthio)[n]staffanes ([**n**]**3**, n = 1,2), generated in situ from the isovalent species [**n**]**2**, have been presented elsewhere.[6] In this paper, we describe the formation of self-assembled monolayers of neat [n]staffane-3,3$^{(n-1)}$-dithiols ([**n**]**4**), thiol-thiol acetates (monothiols, [**n**]**5**), and thiol-ruthenium pentaammine thiols ([**n**]**6**) (Figure 1) on gold electrodes (n = 1-4), as well as mixed films formed with n-alkanethiols. We find that careful basic hydrolysis converts films of [**n**]**5** undamaged

* To whom correspondence should be addressed.

[†] Present address: AT&T Bell Labs, Allentown, PA 18103.

[‡] Present address: Unilever Research, Port Sunlight Laboratory, Quarry Road East, Bebington, Wirral L63 3JW, England.

[§] Present address: Chemistry Department, The Royal Veterinary and Agricultural University, DK-1871 Frederiksberg, Denmark.

[∥] Present address: Institute I, Roskilde University, DK-4000 Roskilde, Denmark.

[⊥] Present address: Department of Chemistry and Biochemistry, University of Colorado, Boulder, CO 80309-0215.

(1) (a) Kaszynski, P.; Michl, J. *J. Am. Chem. Soc.* **1988**, *110*, 5225. (b) Kaszynski, P.; Friedli, A. C.; Michl, J. *Mol. Cryst. Liq. Cryst. Lett. Sect.* **1988**, *6*, 27.

(2) Michl, J.; Kaszynski, P.; Friedli, A. C.; Murthy, G. S.; Yang, H.-C.; Robinson, R. E.; McMurdie, N. D.; Kim, T. In *Strain and Its Implications in Organic Chemistry*; de Meijere, A., Blechert, S., Eds.; NATO ASI Series; Kluwer Academic Publishers: Dordrecht, The Netherlands, 1989; Vol. 273, p 463.

(3) Friedli, A. C.; Kaszynski, P.; Michl, J. *Tetrahedron Lett.* **1989**, *30*, 455.

(4) Kaszynski, P.; Friedli, A. C.; Mich, J. *J. Am. Chem. Soc.* **1992**, *114*, 601.

(5) (a) Bunz, V.; Polborn, K.; Wagner, H.-V.; Szeimes, G. *Chem. Ber.* **1988**, *121*, 1785. (b) Wiberg, H. B.; Waddell, S. T. *J. Am. Chem. Soc.* **1990**, *112*, 2194.

(6) (a) Michl, J.; Friedli, A. C.; Obeng, Y. S.; Bard, A. J. *Proceedings of the Sixth International Conference on Energy and Electron Transfer*; Fiala, J.; Pokorny, J., Eds.; Charles University: Prague, Czechoslovakia, 1989. The rates reported in this paper are too high due to the use of an erroneous literature equation for data treatment. The correct rate constants are 1×10^7 and 2×10^6 s^{-1} for [**1**]**3** and [**2**]**3**, respectively, in 0.1 M DCl in D_2O. (b) Positions on the individual bicyclo[1.1.1]pentane cages in an [n]staffane are distinguished by the number of primes, from no primes at one of the terminal cages to $n-1$ primes on the other terminal cage. Thus, the terminal bridgehead positions in [2]staffane are 3 and 3′, in [3]staffane, 3 and 3″, and in [n]staffane, 3 and 3 with $n-1$ primes, indicated by 3$^{(n-1)}$, following the usage common in mathematics.

0002-7863/92/1514-9943$03.00/0